

National Radio Astronomy Observatory
Socorro, New Mexico

VLA Electronics Memo No. 233

The VLA Installation of the Former Millimeter Array Site Testing Interferometer

Galen Watts
March 1999

Introduction:

This memo outlines the installation of the former Millimeter Array Site Testing Interferometer at the Very Large Array and provides some service procedures that may be necessary for the instrument's proper operation. For a description of the concept behind the instrument, the internal signal path and components, the data processing and expected performance the reader should consult 'Site Test Interferometer' by Radford, Reiland and Shillue, included as appendix A to this memo.

Installation Description:

The site testing interferometer is installed along the east arm of the Very Large Array. The antennas are on a baseline of 300 meters with the western antenna across the access road from VLA antenna pad E4 and the eastern antenna across the access road and approximately 30 meters west of VLA antenna pad E8. The central electronics station is located in a military grade microwave communications shelter across the access road from VLA antenna pad E6. The shelter is attached to a concrete pad and supplied with electric and telephone utilities and an optical fiber linking the interferometer computer to the NRAO network. The antennas are supplied with a local oscillator reference signal and return the first IF signal through a pair of low loss hard line cables for each antenna run in sealed 4 inch PVC conduit buried approximately 4 feet below grade from the shelter to each interferometer antenna. The antennas are commercially available 1.8 meter offset feed satellite television dishes using television low noise block converters modified by the supplier to accept an external local oscillator. The antennas are attached to fixed position mounts in turn attached to concrete pads. On the back of the antennas are weather tight boxes containing direct reference oscillators and voltage regulation for the low noise block converters.

The central electronics shelter contains the interferometer back end and the computer for data logging and communicating the data to the NRAO computer network. The back end is housed in a metal enclosure containing the power supplies and the RF sections beyond the first IF conversion stage. A block diagram of the interferometer including the back end is shown as figure 1 in appendix A (Radford et al) and a layout diagram is shown in G. Reiland's drawing of 14 February 1999 titled 'Electronics Box, mmA' included in appendix B of this memo. The back end supplies two analog signals of approximately 5 kHz at 2.0 Vrms to the computer and the analog conversion card contained within. These voltages and other control and monitoring signals are carried on a 50 conductor ribbon

cable running between the back end enclosure and the computer. There is an AC power interrupter device for remotely restarting the computer and the interferometer back end that is operated by the telephone line. Operation of the AC power interrupter is described in appendix C to this memo.

Adjustment and Repair Notes

Adjusting the Analog Voltage Levels:

The analog voltage levels sent to the computer from the interferometer back end should be nominally 2.0 volts RMS. Currently (March, 1999) the computer shows the voltage over time in a window towards the bottom of the screen.

The adjustment points for the two analog voltages are located on the data acquisition circuit board located near the rear-center of the back end electronics box. The layout diagram labels this circuit board as 'DATA ACQ. PCB', and a parts layout of the data acq. board is shown on drawing DATAAQ_P.DWG in appendix B. On this board are two trimmer potentiometers. Voltage A is adjusted by trimmer R30 located on the side of the circuit board farthest from the front panel of the electronics box, and voltage B is adjusted by trimmer R35 located at the front-right of the circuit board. These trimmers should be adjusted until the voltage on the computer screen is nominally 2.0 volts and both A and B voltages are very close to the same level. Interferometer operation will not be affected if the voltages are not exactly equal, but the voltages should be close to 2.0 volts for the interferometer to operate properly. A voltage variation over time of +/- 0.5 volts has not shown any detrimental effect to interferometer operation.

Monitoring of the Downlink Signal:

The down converted downlink signal from the antennas can be monitored with a spectrum analyzer by disconnecting the IF 1 or IF 2 cable from the side of the electronics cabinet and directly connecting the cable to the analyzer. If IF 1 is used to monitor the signal a splitter or coupler should be installed in line with the IF 1 signal so the signal can be sent both to the analyzer and the IF 1 input so the PLL has a signal to lock on to and will not be sweeping during monitoring. For satellite G-Star 4 the interferometer locks on the CW beacon at an IF frequency of 976 MHz. A plot of the IF spectrum of G-Star 4 c.1997 is included in appendix B.

Testing the Analog Inputs to the Computer:

To test the computer analog inputs a test board is stored in the interferometer shelter in an anti-static plastic bag. This board measures approximately 1 by 4 inches and plugs into the electronics end of the 50 conductor ribbon cable after the cable is disconnected from the electronics box. Care must be taken to insure that pin 1 of the board goes to pin one of the cable. Once the board is plugged into the cable the display on the computer should read approximately 2.0 volts for both the A and B channels. Once the analog inputs have been verified to be operating correctly the board should be removed from the cable and the cable reconnected to the electronics box.

Adjustment of the Phase-Locked Loop Oscillator:

At the time of this writing the phase locked loop had required no adjustment since the time of the original VLA installation of the interferometer (c. 1997). It is suggested that if it is determined that adjustment of the PLL is necessary that the engineer who originally designed and constructed the interferometer, George Reiland, NRAO-Tucson, be consulted before any adjustment attempts. What follows is a summary of George's notes of 25 March 1995 regarding PLL adjustment. These notes are included in their entirety in appendix B.

The PLL circuit board is located in the left rear of the electronics box. Drawing LKBXP2.DWG/ Maser Link PLL shows a parts layout of the PLL board and drawing LKBXREVC.DWG/MaserLink PLL shows a schematic diagram of the PLL. On the circuit board are two trimmer potentiometers, R10 and R12 located to the rear of the PLL circuit board.

Turning R10 ccw (as viewed from above) increases the noise across the band.

Turning R10 cw decreases the noise but breaks lock.

Turning R12 cw increases the noise slightly but makes the lock more stable at lower input power from the front end.

Appendix A:
'Site Test Interferometer'
Radford, Reiland, Shillue
February, 1996

Site Test Interferometer

SIMON J. E. RADFORD, GEORGE REILAND, AND BILL SHILLUE

National Radio Astronomy Observatory, 949 North Cherry Avenue, Tucson, Arizona 85721-0665

Electronic mail: (sradford, greiland, bshillue)@nrao.edu

Received 1995 October 26; accepted 1996 February 19

ABSTRACT. To evaluate possible sites for NRAO's proposed Millimeter Array, we constructed interferometers to measure directly the tropospheric phase stability. These instruments observe an unmodulated 11.5 GHz beacon broadcast from a geostationary satellite and measure the phase difference between the signals received by two antennas 300 m apart. Because the atmosphere is non-dispersive away from line centers, the results can be scaled to millimeter and submillimeter wavelengths. Novel design features of the instruments include a local oscillator phase locked to the received signal and digital correlation of the downconverted signals with a computer. Two instruments have been deployed, one at 3720 m on Mauna Kea, Hawaii, and the other at 5000 m near Cerro Chajnantor in northern Chile. With identical instruments operating simultaneously, we can directly compare the phase stability at the two sites.

1. INTRODUCTION

By altering the refractive index, inhomogeneously distributed atmospheric water vapor causes spatial and temporal variations in the electrical path length for radio waves. Path-length differences across a telescope aperture distort the incoming wave front and present natural limits to the angular resolution and sensitivity of astronomical observations. These limits can be particularly onerous at millimeter and submillimeter wavelengths. Both the total amount and the turbulence of the water vapor over a telescope are determined by the local site topography and climate (Masson 1993). Although active techniques can correct atmospheric distortions to some degree, it behooves planners of a new instrument to choose a site with the best possible natural resolution limits.

The NRAO has proposed to build the Millimeter Array (MMA), an interferometer with forty 8-m diameter antennas for observations at frequencies of 30–350 GHz on baselines of 15 m–3 km (Hughes 1990). To evaluate possible sites for this instrument, we have built small-aperture interferometers to measure atmospheric wave-front distortions. Each instrument observes a beacon broadcast from a geostationary communications satellite and measures the phase difference between the signals received by two antennas 300 m apart. Although the beacon frequency is around 11.5 GHz, the results can be scaled to at least 350 GHz (Hills 1995) because the atmosphere is nondispersive away from line centers (Liebe 1989).

Our instrument is based on earlier work by Ishiguro et al. (1990), by Ishiguro et al. (1993), and by Masson (1994). Novel features of our design include a local oscillator phase locked to the signal received at one antenna, and digital correlation of the downconverted signals with a computer. Two instruments have been deployed, one at 3720 m on Mauna Kea, Hawaii, and the other at 5000 m near San Pedro de Atacama in northern Chile.

2. DESIGN CONSIDERATIONS

Geostationary communications satellites are convenient sources for atmospheric sounding because they broadcast strong, stable signals from fixed celestial locations. Since the precision of a phase measurement approximately equals the voltage signal-to-noise ratio (Thompson et al. 1986) and since path-length fluctuations correspond to phase fluctuations that scale with frequency, a higher signal-to-noise ratio is necessary at lower frequencies. On the other hand, receivers generally perform better, components are cheaper, and satellite broadcasts are more plentiful at lower frequencies. The first site test interferometer used a 19 GHz beacon (Ishiguro et al. 1990), but subsequent instruments, including ours, have all used Ku band broadcasts around 11.5 GHz.

Although modulated signals can be used as wide-band noise sources and correlated without regard to their information content, this would require expensive, specialized correlator hardware. By contrast, unmodulated carriers can be either correlated with a vector voltmeter or digitized and correlated with a computer. Fortunately, a few geostationary satellites do broadcast unmodulated Ku band beacons. The GTE Gstar satellites broadcast pilot signals to the continental United States and Hawaii for mobile uplinks. Many Intelsats have omni-directional beacons visible throughout the sub-satellite hemisphere.

Phase decorrelation causes exponential sensitivity loss in an interferometer, $\propto 1 - \exp(-\sigma^2/2)$, where σ is the rms phase jitter (Thompson et al. 1986). At 350 GHz, rms phase fluctuations of 10° , or path length fluctuations of $24 \mu\text{m}$, will cause a negligible loss of sensitivity, 1.5%. Greater phase jitter will make coherent observations increasingly difficult without active phase correction, so our design goal was to measure atmospheric path-length fluctuations of this magnitude. For beacon frequencies around 11.5 GHz, rms path-length fluctuations of $25 \mu\text{m}$ correspond to phase fluctuations of 0.33° . Hence the necessary voltage signal-to-noise ratio is 175, or 45 dB in power.

The dependence of phase fluctuations on separation, s , is

characterized by the structure function, $D_\phi(s) = \langle |\phi(x) - \phi(x+s)|^2 \rangle$, where $\phi(x)$ is the atmospheric phase at position x (Tatarski 1961). For separations of tens or hundreds of meters, this has an approximately power-law form, $D_\phi(s) \approx D_\phi(s_0)(s/s_0)^{2\alpha}$, with an exponent $1/3 \leq \alpha \leq 5/6$. The extremes represent, respectively, two- and three-dimensional Kolmogorov turbulence. So for a given sensitivity, an instrument with a longer baseline can measure atmospheric phase fluctuations under better conditions. Conversely, maintaining instrumental phase stability is harder for longer baselines. To directly sample phase fluctuations on baselines relevant for the MMA, we designed our interferometers with a nominal baseline of 300 m, which is slightly larger than the geometric mean of the MMA's 15m–3 km baselines. This choice was influenced by the availability of an unused underground utility conduit with access holes every 150 m along the road to the VLBA site on Mauna Kea.

Geostationary satellites are normally maintained by periodic station keeping so their diurnal motions take them less than 0.1° from their assigned positions. To avoid the complexity of phase stably tracking a moving satellite, we chose antennas small enough that their beams are much larger than the diurnal satellite motion. At 12 GHz, a 1.8 m antenna has an Airy pattern of 1° diameter, making tracking unnecessary. This desire to avoid tracking would also rule out astronomical sources, even if they were strong enough. On the other hand, only one sight line through the atmosphere is probed with a geostationary source.

We are interested in time scales from seconds up to about 15 min, which is several times longer than the time taken for an atmospheric parcel to blow across the interferometer at typical winds speeds. Hence any thermal drifts in the instrument could vary only slowly on these time scales. We relied mostly on passive techniques to achieve this, with some critical components, namely the first local oscillators, thermally stabilized actively. The post-detection bandwidth of 2 Hz (1-s integration intervals) is a compromise between an adequate signal-to-noise ratio and interest in the shortest time scales.

3. COMPONENTS

The 1.8-m diameter, offset feed antennas are molded from glass fiber reinforced polyester with an embedded metallic mesh (Prodelin: Conover, NC). They are mounted on steel azimuth-elevation positioners attached to concrete foundations. We modified the standard positioners to increase their transverse (cross elevation) stiffness and resistance to wind loads.

The local oscillator reference and received IF signals are transmitted between the antennas and the central electronics station along 13-mm diameter Heliax cable (Andrew: Orland Park, IL). This cable has a foam polyethylene dielectric and has been thermally cycled to stabilize its phase change with temperature. In addition, it is buried, either directly (Chile) or in conduit (Hawaii), and the short runs above ground are insulated to minimize both the total diurnal temperature variation and the rate of change of temperature. Separate cables are used for the LO reference and the IF signals.

The interferometer employs three stages of downconver-

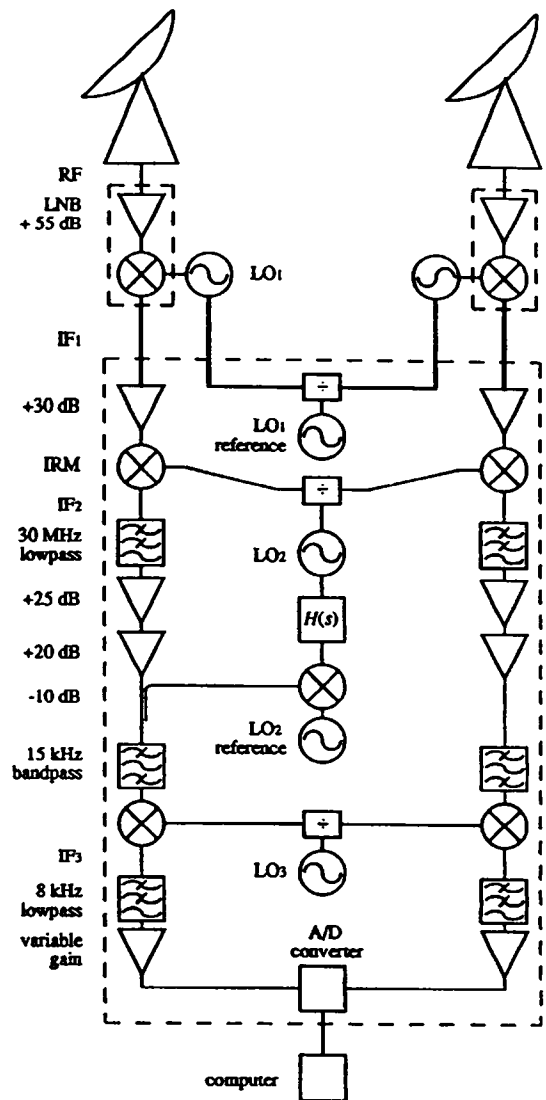


FIG. 1—Block diagram of the site test interferometer.

sion (Fig. 1). Low noise communications receivers (LNBs; Gardiner: Garland, TX) amplify the Ku band rf signals and downconvert them to an L band IF_1 (Table 1). These receivers were modified to accept an external LO signal generated by temperature stabilized, dielectric resonant oscillators phase locked to a common temperature-stabilized crystal oscillator. The high LO_1 reference frequency, 298.6111 MHz, was chosen to minimize the sensitivity to phase fluctuations.

The IF_1 signals are amplified, downconverted to 21.4 MHz with an image rejection mixer, and further amplified. The second LO is phase locked to one of the received signals and to a 21.4 MHz crystal reference oscillator. The IF_2 signals pass through 15 kHz crystal filters and are then mixed down to the final $IF_3 = 5$ kHz. The third LO is a crystal oscillator. The 15 kHz bandwidth is a compromise between increased signal-to-noise ratio and decreased phase stability; narrower filters might be expected to have larger phase-temperature coefficients and, worse, poorer phase-temperature tracking between the two channels. The 5 kHz signals are finally amplified to roughly ± 4 –5 V peak-to-peak (2–3 V rms) and filtered with an 8 kHz low pass anti-aliasing filter. The downconversion and amplifier chain is not calibrated in amplitude.

TABLE I
NRAO Site Test Interferometers

		Mauna Kea, Hawaii (VLBA)	Cerro Chajnantor, Chile
Site	Latitude	19° 48' 16" N	23° 1' 4" S
	Longitude	155° 27' 29" W	67° 45' 7" W
	Altitude	3720 m	5000 m
	Datum	Old Hawaiian 1866	South American 1956
Baseline	Azimuth	56°	90°
	Length (optical)	281 m	285 m
	Length (electrical)	311 m	305 m
Satellite		GTE Gstar 4	Intelsat 601
	Orbital Longitude	105° W	27.5° W
	Elevation	29°	36°
	Azimuth	106°	65°
	Beacon	11.7269 GHz	11.1980 GHz
	Polarization	linear	right hand circular
Antenna	Diameter	1.8 m	1.8 m
	Gain	46.5 dB	46.5 dB
	Noise Temperature	35 K	35 K
LNB	Noise Figure	0.7 dB	0.6 dB
	Gain	59 dB	55 dB
Oscillators	LO ₁ reference	298.611 MHz	298.611 MHz
	LO ₁	10750.00 MHz	10152.77 MHz
	LO ₂ reference	21.400 MHz	21.400 MHz
	LO ₂	955.5 MHz	1023.8 MHz
	LO ₃	21.395 MHz	21.395 MHz
Signal	IF ₁	976.9 MHz	1045.2 MHz
	LNB Output	-56 ± 1 dBm	-69 ± 1 dBm
	Noise at LNB Output	-125 dBm Hz ⁻¹	-125 dBm Hz ⁻¹
	signal/noise	69 dB Hz ⁻¹	56 dB Hz ⁻¹
	Inferred EIRP	14 dBW	6 dBW
	IF ₂	21.400 MHz	21.400 MHz
	IF ₃	5 kHz	5 kHz

The receiver feeds are linearly polarized, as are the beacons on the Gstar satellites. Since the Intelsat beacons are, however, circularly polarized, we mounted meander-line polarizers in front of the feed horns to maximize the received signals. These polarizers consist of four thin printed circuits spaced about one quarter wavelength apart with low loss foam in between. The circuits themselves are etched copper meander line patterns on a flexible substrate (Young et al. 1973).

4. DATA PROCESSING

The IF₃ signals are digitized at 20 ksamples s⁻¹ channel⁻¹ with a 12 bit analog-to-digital converter. The converter actually runs at 40 ksamples s⁻¹, alternatively sampling the two channels. Hence the two sample streams are skewed by 25 μs and they must be synchronized before they are correlated. In addition, a quadrature signal is needed to extract the relative phase independent of amplitude variations. Both these operations are implemented with finite response digital filters.

Let $A(t_{2i})$ and $B(t_{2i+1})$ represent the two data streams, alternately sampled at times $t_i = i\Delta t$, where the sampling interval $\Delta t = 25 \mu\text{s}$. Since any offsets in the sampled signals would cause an error in the measured phase, the mean values

are first subtracted from the data streams, $\hat{A}(t_{2i}) = A(t_{2i}) - \langle A \rangle$ and $\hat{B}(t_{2i+1}) = B(t_{2i+1}) - \langle B \rangle$. The ensemble averages denoted by $\langle \rangle$ are implemented as time averages over 1 s intervals. Then the sum and difference streams $\bar{B}(t_{2i}) = [\hat{B}(t_{2i-1}) + \hat{B}(t_{2i+1})]/2$ and $B'(t_{2i}) = [\hat{B}(t_{2i-1}) - \hat{B}(t_{2i+1})]/2$ are identically 90° out of phase for all frequencies and are time synchronous with A . They have, however, different frequency responses; \bar{B} is insensitive to high frequencies and B' is insensitive to low frequencies. Over the Nyquist interval, $\bar{B} \propto \cos(\pi f/2f_N)$, and $B' \propto \sin(\pi f/2f_N)$, where $f_N = 10 \text{ kHz}$ is the Nyquist frequency. We put the final IF₃ at $f_N/2 = 5 \text{ kHz}$, where \bar{B} and B' have equal response.

The phase, ϕ , is determined from the complex correlation coefficient,

$$\phi = \arg\left\{ \frac{\langle \hat{A}\bar{B} \rangle}{(\langle \hat{A}^2 \rangle \langle \bar{B}^2 \rangle)^{1/2}} + i \frac{\langle \hat{A}B' \rangle}{(\langle \hat{A}^2 \rangle \langle B'^2 \rangle)^{1/2}} \right\}.$$

The phase time series is written to a file every 60 s along with status information and simple statistics. Each block of sixty 1 s phases is perfectly synchronous, i.e., no samples are lost, and the gaps between the blocks are a few × 10 ms. Data summaries are transmitted by fax to our offices once or twice daily from each site. These include cumulative distributions of the rms phases over 60-s intervals. The raw data

are copied to tape and retrieved every month or two for further analysis (Holdaway et al. 1995).

The data acquisition and processing software was written with the LabView graphical programming system (National Instruments: Austin, TX) and runs under Windows (Microsoft: Redmond, WA) on a '486 computer (Gateway: Sioux City, SD). The calculations are done with floating point numbers. Even though they could be recast in faster, integer arithmetic, this is unnecessary since the data-processing throughput is limited by the acquisition hardware, not the calculation speed.

5. FIELD DEPLOYMENTS AND MEASURED PERFORMANCE

Two instruments have been constructed. The first was deployed in 1994 September at 3720 m altitude near the VLBA antenna on Mauna Kea, Hawaii. A similar interferometer with a 100 m baseline is installed at 4000 m near the JCMT (Masson 1994) and 225 GHz tipping radiometers are installed both at the CSO, adjacent to the JCMT, and at the VLBA site (Brown and Schwab 1995).

On Hawaii, the interferometer receives the Gstar 4 beacon (Table 1). At the output of the first downconverter, the measured power signal-to-noise ratio is 69 dB Hz^{-1} . This is maintained throughout the IF chain. Before deployment, the instrument performance was evaluated by placing the two antennas next to each other. With a separation of only a few meters, there is virtually no atmospheric contribution to the observed phase fluctuations. These tests consistently showed minimum rms phase fluctuations of 0.2° , or $15 \mu\text{m}$, over 60-s intervals.

The second interferometer was deployed in 1995 April–May at 5000 m altitude near Cerro Chajnantor in northern Chile. It is installed together with a 225 GHz tipping radiometer and a weather station. This site is near the village of San Pedro de Atacama, about 275 km ENE of Antofagasta. The equipment there has a solar and wind power system and an Inmarsat satellite telephone. This interferometer receives the beacon on Intelsat 601. With the polarizers installed on the feeds, the measured power signal-to-noise ratio is 56 dB Hz^{-1} .

A sample time series of phases and fluctuations observed at the end of 1995 June at Cerro Chajnantor (Fig. 2) illustrates the performance of the instruments. Diurnal and other components of the satellite motion cause large swings in the interferometer phase that must be filtered out during data processing (Holdaway et al. 1995). Diurnal variations of the phase fluctuations are also evident: the atmosphere is quieter at night than during the day (local noon is about 16^{h} UT). The cumulative distribution for 1995 June (Fig. 3) shows the median rms phase fluctuation was about $120 \mu\text{m}$. This corresponds to 32° at 240 GHz, implying interferometric observations with $1''$ resolution at that frequency (300 m baseline) were possible about 50% of the time without active phase correction. These data are typical of good conditions at this site.

With identical instruments operating simultaneously, we can directly compare the phase stability at Mauna Kea and at Cerro Chajnantor. Preliminary results of this ongoing com-

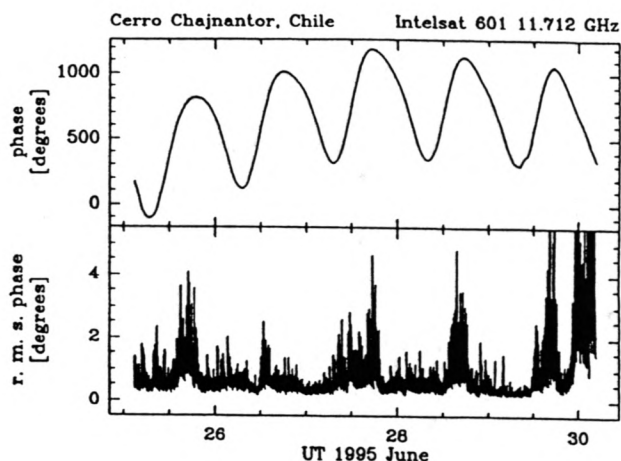


FIG. 2—Sample time series of interferometer phase measurements at Cerro Chajnantor, Chile. These data are typical of good conditions there. *upper*: Interferometer phase; averages of 1-s measurements over 60-s intervals. *lower*: Phase fluctuations; rms of 1-s measurements over 60-s intervals.

parison can be viewed at <http://www.tuc.nrao.edu/mma>. We have also compared our data with archival data for other sites, notably “millimeter valley” near the summit of Mauna Kea (Masson 1994). Although it is premature to draw firm conclusions about the sites, since those require measurements extending over several seasons, initial results for Mauna Kea indicate the phase-stability distributions are similar at the VLBA site and at millimeter valley, but the best conditions can occur at different times at these two locations. We confirm the pronounced diurnal variation in the phase stability at Mauna Kea. At Cerro Chajnantor, the phase stability appears substantially better than at Mauna Kea. The diurnal variation is less pronounced and conditions of good phase stability occur two to three times more often.

Darrel Emerson, John Payne, and Dick Thompson sketched out the instrument’s design in the spring of 1993. Bill Hancock, Mike Prater, and Tony Sylvester, in Hawaii, and Angel Otárola, in Chile, were invaluable for the deployments. Mark Holdaway and Scott Foster calculated the cumulative distribution in Fig. 3. Marty Levine, Colin Masson, and Peter Napier shared much helpful advice. The National Radio Astronomy Observatory is a facility of the National

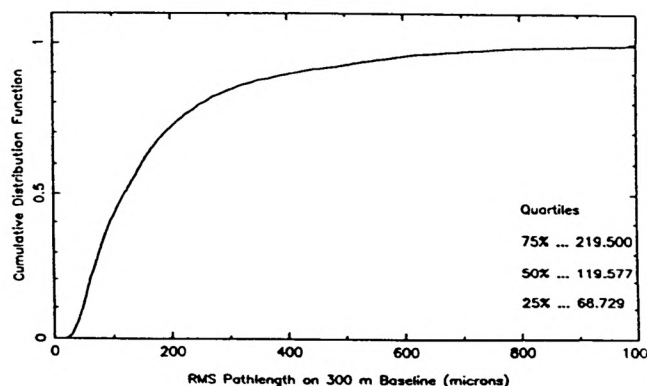


FIG. 3—Cumulative distribution of rms phase fluctuations over 10 min intervals for 1995 June at Cerro Chajnantor, Chile.

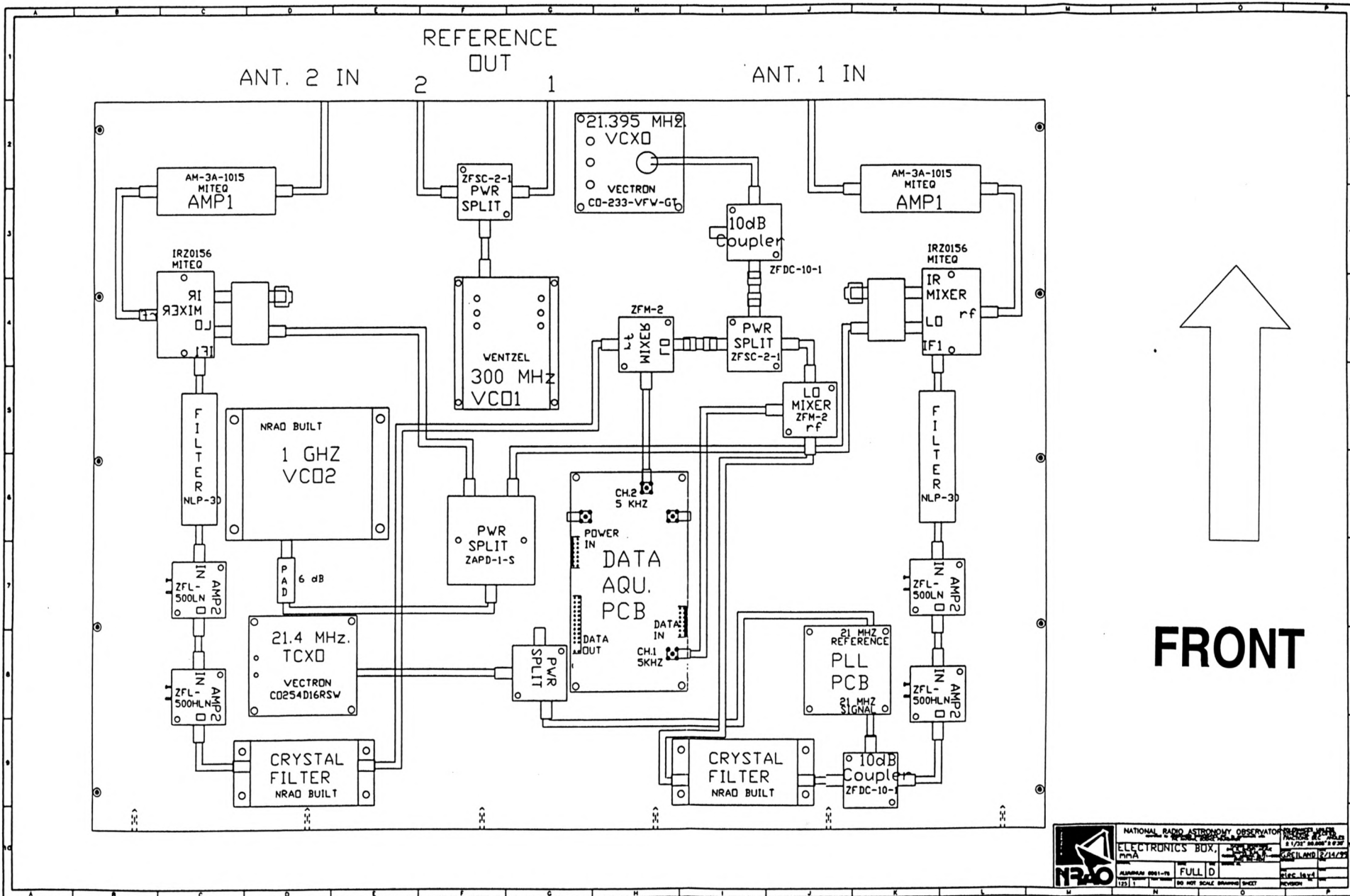
Science Foundation operated under cooperative agreement by Associated Universities, Inc.

REFERENCES

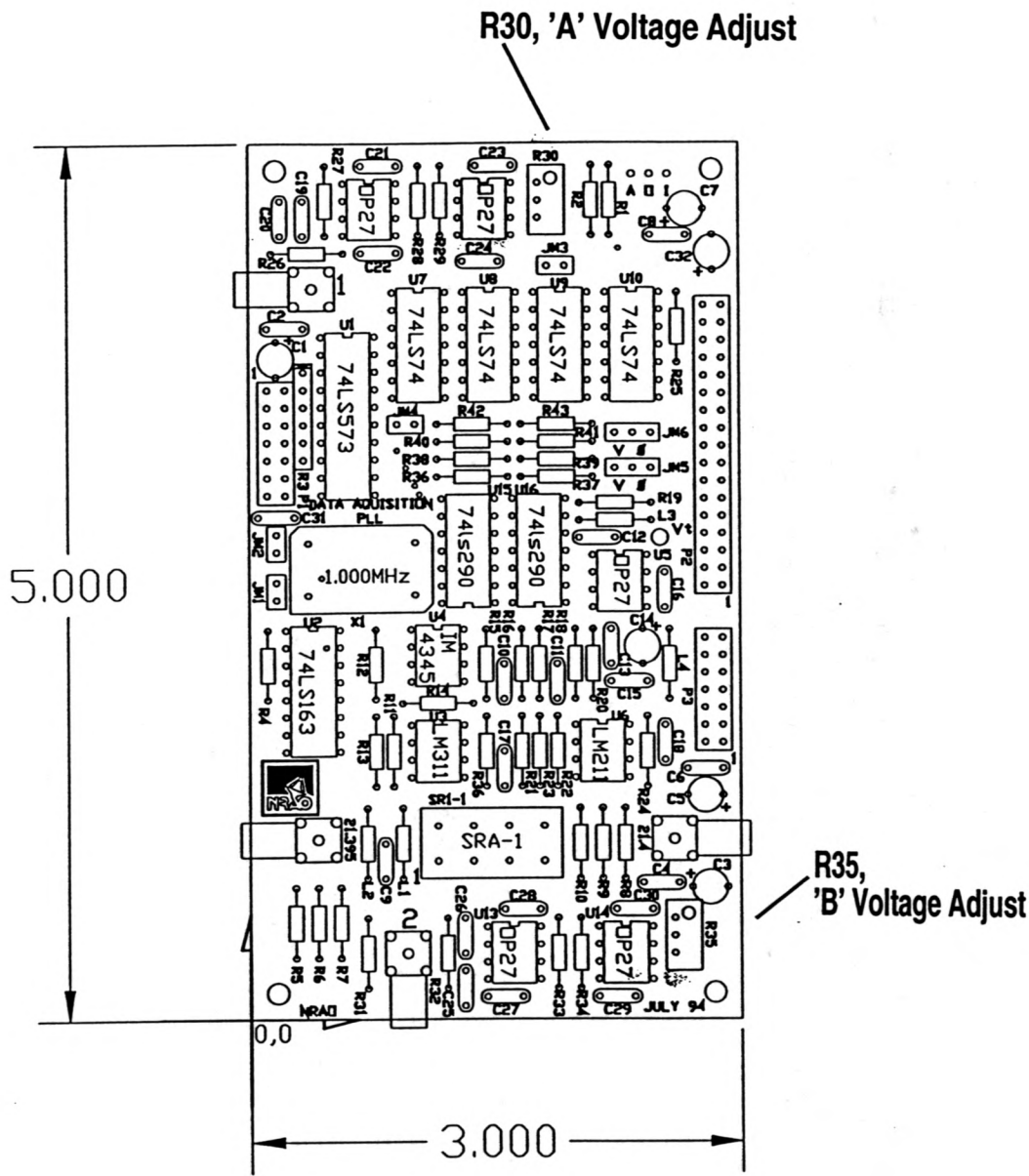
- Brown, R. L., and Schwab, F. 1995, private communication
- Hills, R. E. 1995, private communication
- Holdaway, M. A., Radford, S. J. E., Owen, F. N., and Foster, S. M. 1995, Millimeter Array Memo 129 (Socorro, NM, NRAO)
- Hughes, R. E. 1990, The Millimeter Array, proposal to the National Science Foundation (Washington, DC, AUI)
- Ishiguro, M., Kanzawa, T., and Kasuga, T. 1990, in *Radio Astronomical Seeing*, URSI/IAU Symp., ed. J. E. Baldwin and S. Wang (Beijing, IAP), p. 60
- Ishiguro, M., Kawabe, R., Nakai, N., Morita, K.-I., Okumura, S. K., and Ohashi, N. 1993, in *Astronomy with Millimeter and Submillimeter Wave Interferometry*, IAU Colloq. 140, ed. M. Ishiguro and W. J. Welch (San Francisco, ASP), p. 405
- Liebe, H. J., 1989, *Intl. J. IR & MM Waves*, 10, 631
- Masson, C. R. 1994, in *Astronomy with Millimeter and Submillimeter Wave Interferometry*, IAU Colloq. 140, ed. M. Ishiguro and W. J. Welch (San Francisco, ASP), p. 87
- Masson, C. R. 1993, in *Very High Angular Resolution Imaging*, IAU Symp. 158, ed. J. G. Robertson and W. J. Tango (Dordrecht, Kluwer), p. 1
- Tatarski, V. I. 1961, *Wave Propagation in a Turbulent Medium* (New York, McGraw-Hill)
- Thompson, A. R., Moran, J. M., and Swenson, G. W., Jr. 1986, *Interferometry and Synthesis in Radio Astronomy* (New York, Wiley)
- Young, L., Robinson, L. A., and Hacking, C. A. 1973, *IEEE Trans. Ant. Prop.*, 21, 376

Appendix B:
Drawings and Diagrams

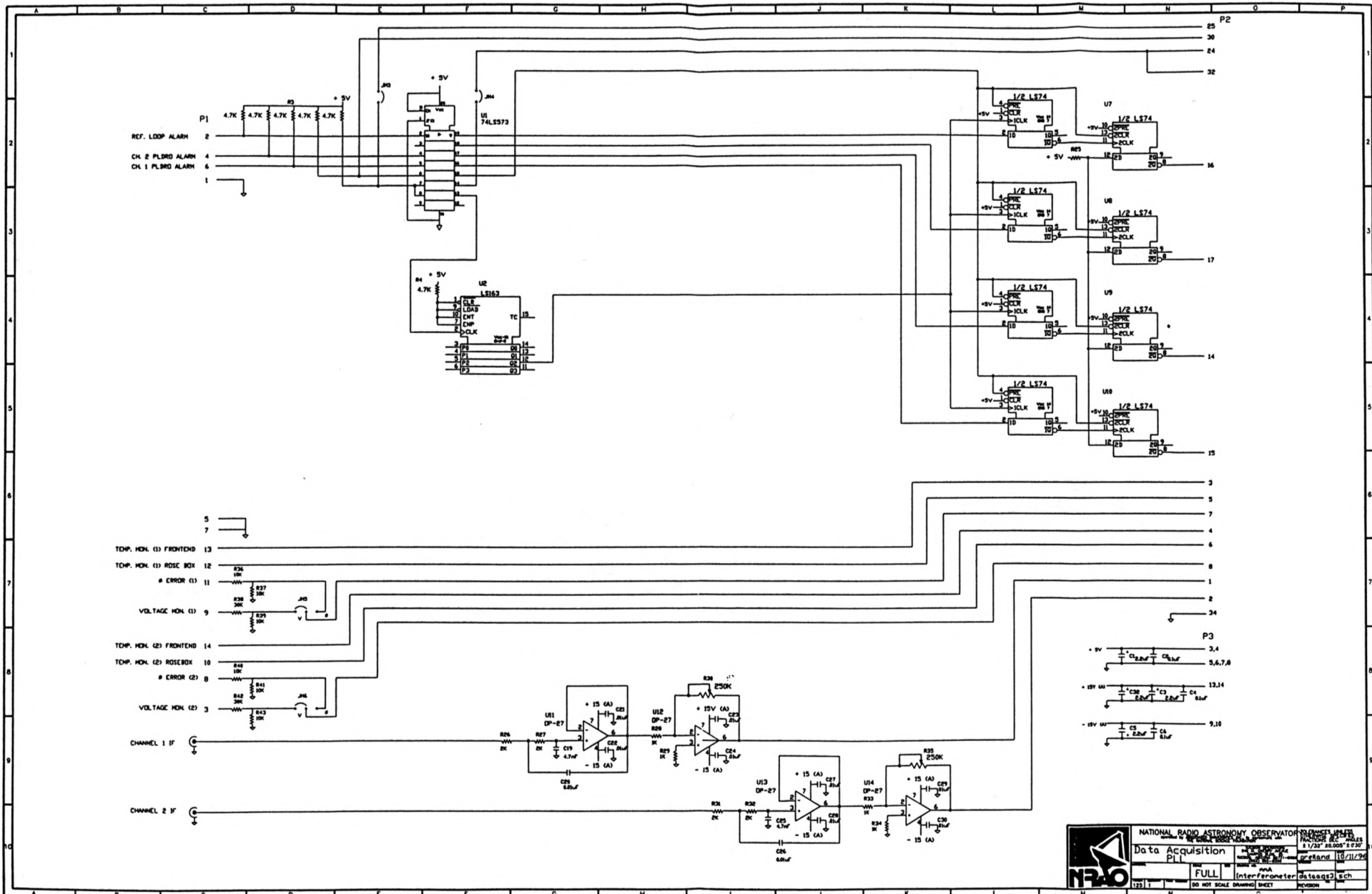
Electronics/RF Layout Diagram
Data Acquisition PC Board Layout
Data Acquisition PC Board Schematic
PLL Board Layout
PLL Board Schematic
RF Block Diagram
Reiland's PLL Notes
IF Spectrum Plots




	NATIONAL RADIO ASTRONOMY OBSERVATORY	PROJECT NAME
	ELECTRONICS BOX	PROJECT NO.
ADDRESS 0811-10	FULL D	DATE
1721	NO NET SCALE DRAWING SHEET	DESIGNED BY



TOLERANCES UNLESS OTHERWISE SPECIFIED FRACTIONS DEC ANGLES ±		NATIONAL RADIO ASTRONOMY OBSERVATORY - TUCSON OPERATIONS operated by ASSOCIATED UNIVERSITIES INC., under contract with THE NATIONAL SCIENCE FOUNDATION		
APPROVALS DRAWN E.D.KEMP CHECKED REVISED		Data Aquisition PLL PC Board		
DATE 9JUN94		SCALE	SIZE B	DRAWING NO. DATAAQ_P.DWG
		DO NOT SCALE DRAWING		SHEET 1 OF 1



	NATIONAL RADIO ASTRONOMY OBSERVATORY	
	Data Acquisition P1	
FULL	Interferometer	dataaqs2.sch
1/25	DO NOT SCALE DRAWING SHEET	INCHES



TOLERANCES UNLESS OTHERWISE SPECIFIED
FRACTIONS DEC ANGLES
±

APPROVALS DATE

DRAWN E.D.KEMP 27JUN95

CHECKED

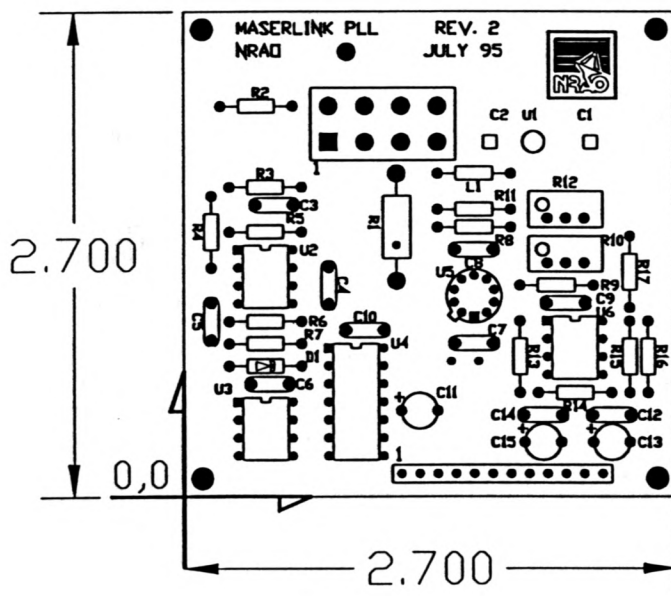
REVISED

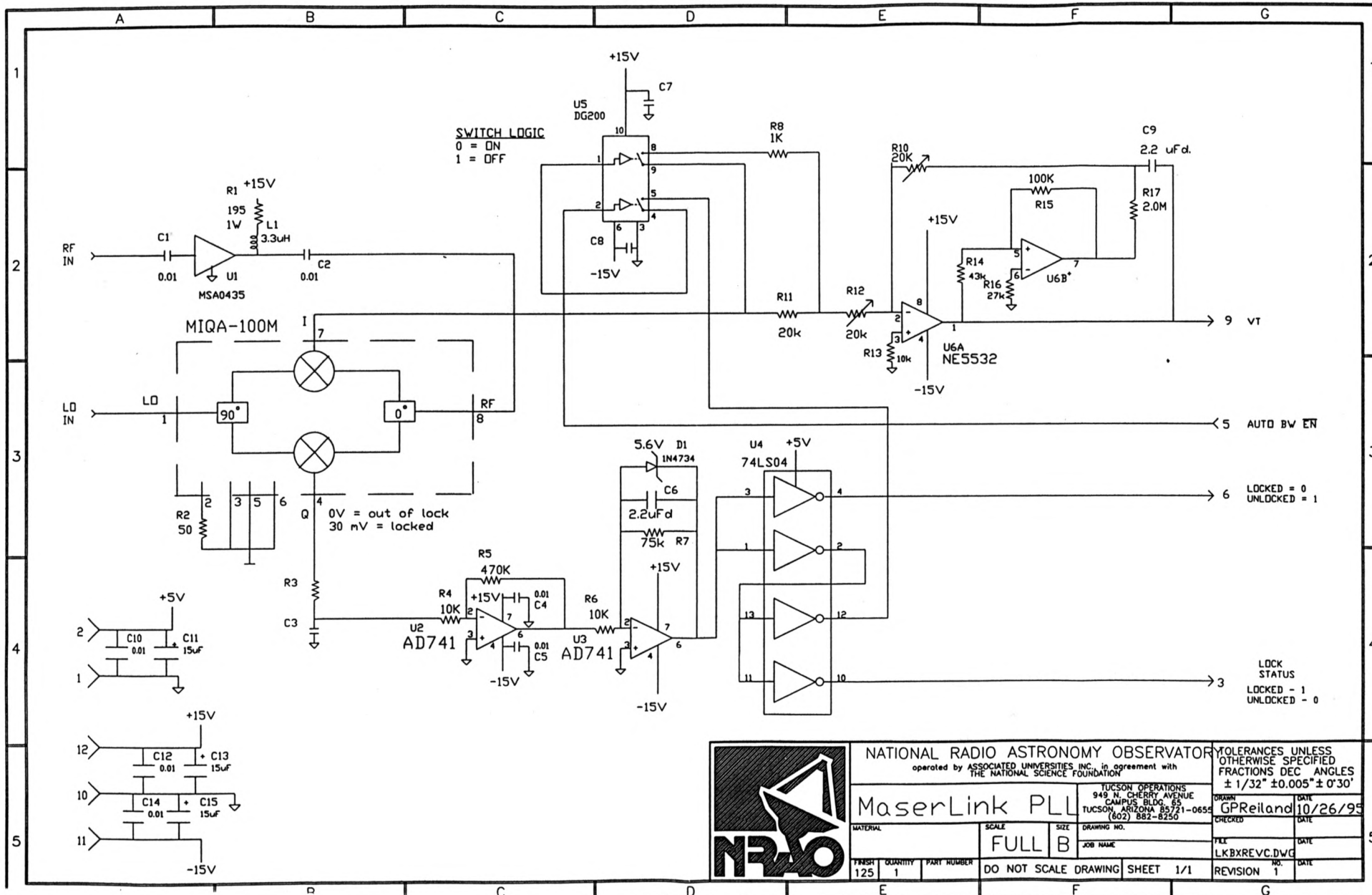
NATIONAL RADIO ASTRONOMY OBSERVATORY - TUCSON OPERATIONS
operated by ASSOCIATED UNIVERSITIES INC., under contract with
THE NATIONAL SCIENCE FOUNDATION

MASER LINK PLL

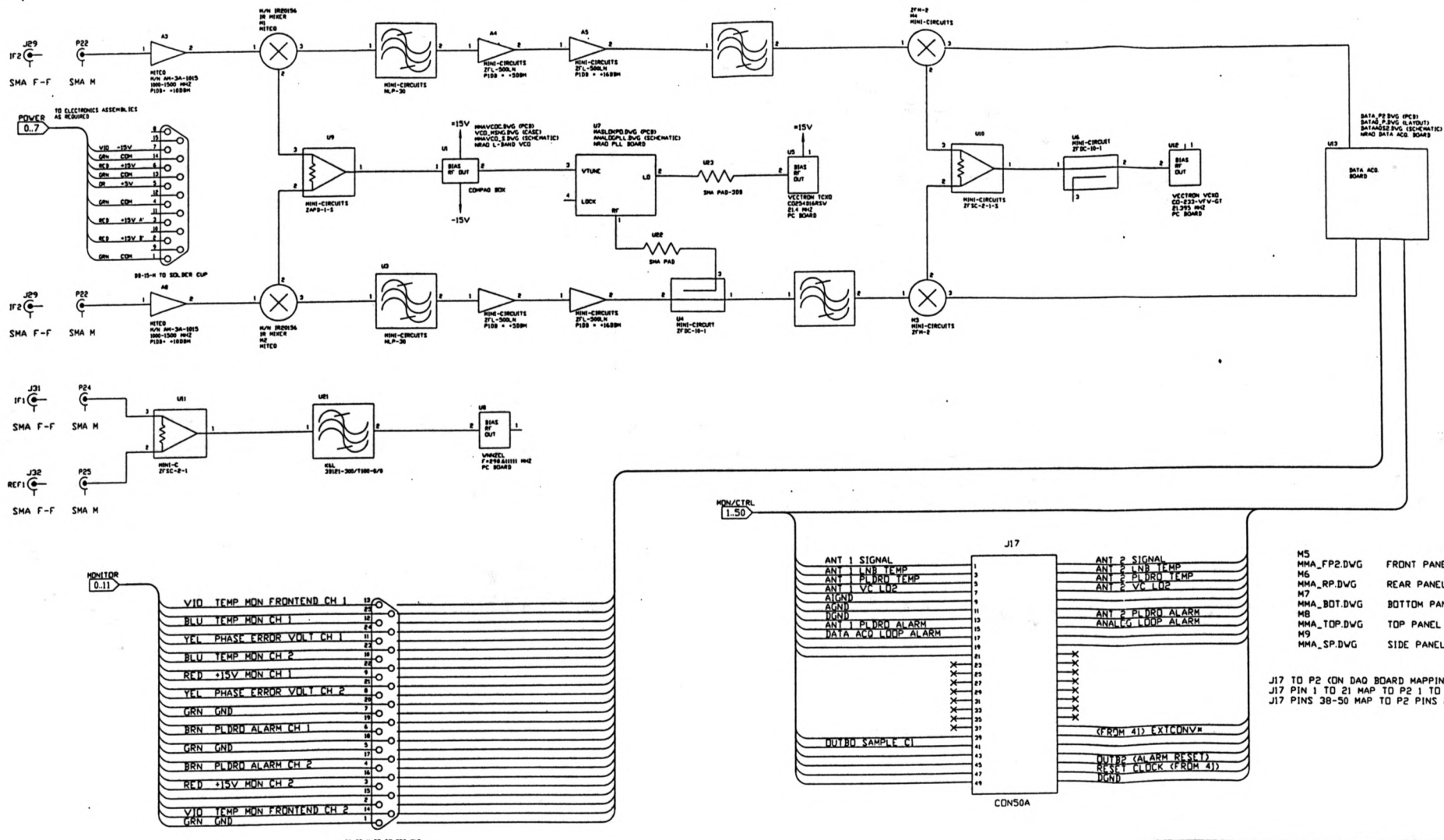
SCALE SIZE DRAWING NO.
B LKBXP2.DWG

DO NOT SCALE DRAWING SHEET 1 OF 1



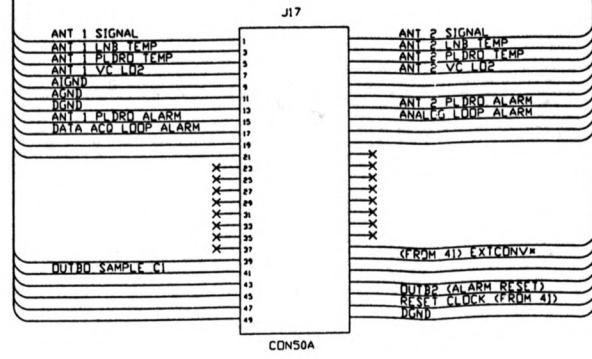


NATIONAL RADIO ASTRONOMY OBSERVATORY <small>operated by ASSOCIATED UNIVERSITIES, INC. in agreement with THE NATIONAL SCIENCE FOUNDATION</small>		<small>TOLERANCES UNLESS OTHERWISE SPECIFIED</small> <small>FRACTIONS DEC ANGLES</small> <small>± 1/32" ± 0.005" ± 0'30"</small>	
MaserLink PLL		<small>TUCSON OPERATIONS</small> <small>949 N. CHERRY AVENUE</small> <small>TUCSON, ARIZONA 85721-0654</small> <small>(602) 882-8250</small>	<small>DRAWN</small> <small>DATE</small> <small>CHECKED</small> <small>DATE</small>
<small>MATERIAL</small> FULL B	<small>SCALE</small> FULL B	<small>SIZE</small> FULL B	<small>FILE</small> LKBXREVC.DWG
<small>FINISH</small> 125	<small>QUANTITY</small> 1	<small>PART NUMBER</small> DO NOT SCALE DRAWING SHEET 1/1	<small>REVISION</small> 1



- M5 MMA_FP2.DWG FRONT PANEL
- M6 MMA_RP.DWG REAR PANEL
- M7 MMA_BOT.DWG BOTTOM PANEL
- M8 MMA_TOP.DWG TOP PANEL
- M9 MMA_SP.DWG SIDE PANEL

J17 TO P2 (ON DAQ BOARD MAPPING)
 J17 PIN 1 TO 21 MAP TO P2 1 TO 21
 J17 PINS 38-50 MAP TO P2 PINS 22-34



TOLERANCES UNLESS OTHERWISE SPECIFIED FRACTIONS DEC ANGLES		NATIONAL RADIO ASTRONOMY OBSERVATORY - TUCSON CAMPUS OPERATED BY ASSOCIATED UNIVERSITIES INC. UNDER CONTRACT TO THE NATIONAL SCIENCE FOUNDATION	
APPROVALS		DATE	
E.D. DEW		APR 12 89	
SCALE		SIZE	
D		DRAWING NO.	
DO NOT SCALE DRAWING		SHEET 1 C	

mA Interferometer - Hawaii Elec. Box 5/25/95

Problem : Locks to modulated carrier @ 982.9 MHz
+ 986.9 MHz

Solution : Limit sweep by adjusting set point of
loop sweep amp.

Change from 47K to 124K

Changed V_t sweep -5V to +5V

Inside testing $\Rightarrow T = 302^\circ K$

w/ $V^- = -15.75V$

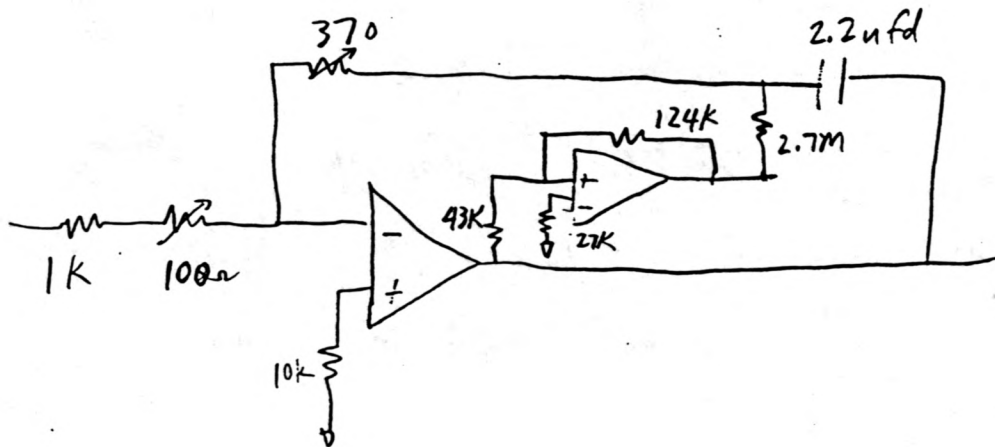
$V_t @ 955.4\text{MHz} = +1.38$

w/ $V^- = -15.0V$

$V_t @ 955.4\text{MHz} = -5.400$

$V^- = -14.5V$

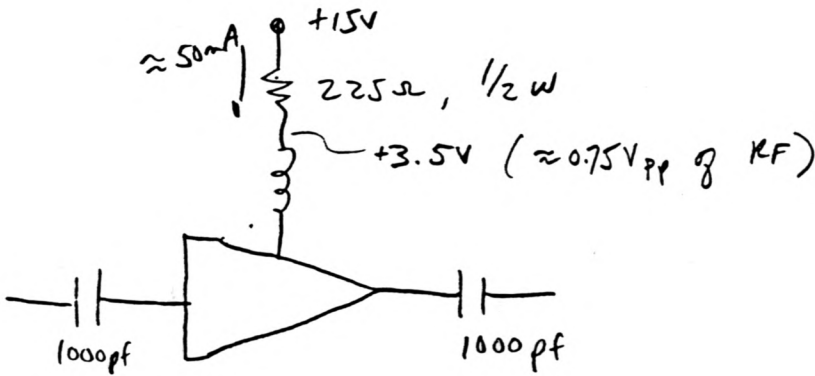
$V_t @ 955.4\text{MHz} = -1.550$



5/25/95

mmA interferometer - Hawaii Box

- Changed bias resistor to INA 02 microstrip amp



Sweep rate = $1/13 \text{ sec}$

" range = $\pm 5 \text{ V}$

Loop Adjustment notes:

$R_3 = \text{feedback } j \text{ } R_2 = \text{input}$
 $= R_{10} \text{ on pcb.} \quad = R_{12} \text{ on pcb.}$

reference is looking into Box from front

TURN R_3 toward front (larger R) the noise increases across the band.

TURN R_3 toward back (lower R) the noise decreases, but breaks lock

TURN R_2 clockwise (smaller R) the noise increases slightly however the lock is more stable @ lower input power from front end.

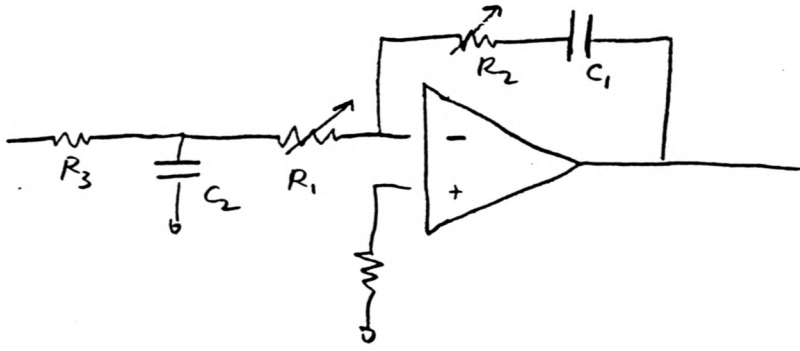
$V_{\text{lock}} = 0.018$ ($R_2 = \phi$) locking from low side
 $R_3 \approx 370 \Omega$

0.033 ($R_2 = 0$) locking from high side
 $R_3 \approx 370$

0.024 $R_2 \approx 100 \Omega$

mmA interferometer PLL

3/29/95



$$K_0 = 1.5 \text{ MHz/V} \Rightarrow 2\pi \times 15 \times 10^6 \text{ rad/Volt/Sec}$$

$$K_d = 400 \text{ mV/rad}$$

if we disregard $R_3 + C_2$, then we have TYPE 2, 2nd order

$$\tau_1 = R_1 C_1 = (7.5K)(0.1\mu F) = 7.5 \times 10^{-4} \quad \tau_2 = R_2 C_1 = (10K)(0.1\mu F) = 1 \times 10^{-3} \quad F(s) = \frac{s\tau_2 + 1}{s\tau_1}$$

$$\omega_n = \left(\frac{K_0 K_d}{\tau_1} \right)^{1/2} = \left(\frac{2\pi \times 15 \times 10^6 \times 0.4}{7.5 \times 10^{-4}} \right)^{1/2} = 2.24 \times 10^5 \text{ rad s}^{-1} \approx 35 \times 10^3 \text{ Hz}$$

$$f = \frac{\tau_2}{2} \left(\frac{K_0 K_d}{\tau_1} \right)^{1/2} = \frac{\tau_2 \omega_n}{2} = (0.5 \times 10^{-3}) (2.24 \times 10^5) = 1.12 \times 10^2$$

$\Delta\omega \Rightarrow$ sweep rate

$$\frac{\Delta\omega}{\omega_n^2} < 0.1$$

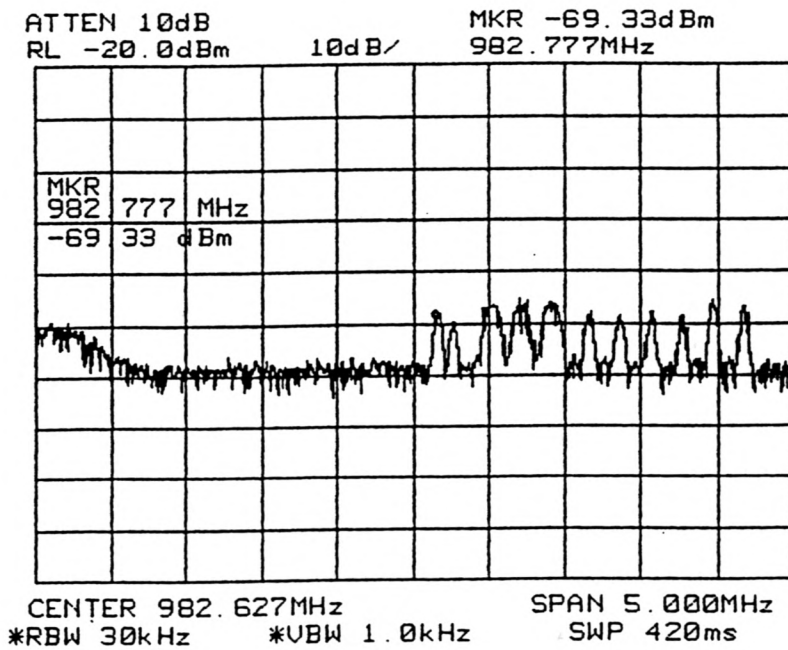
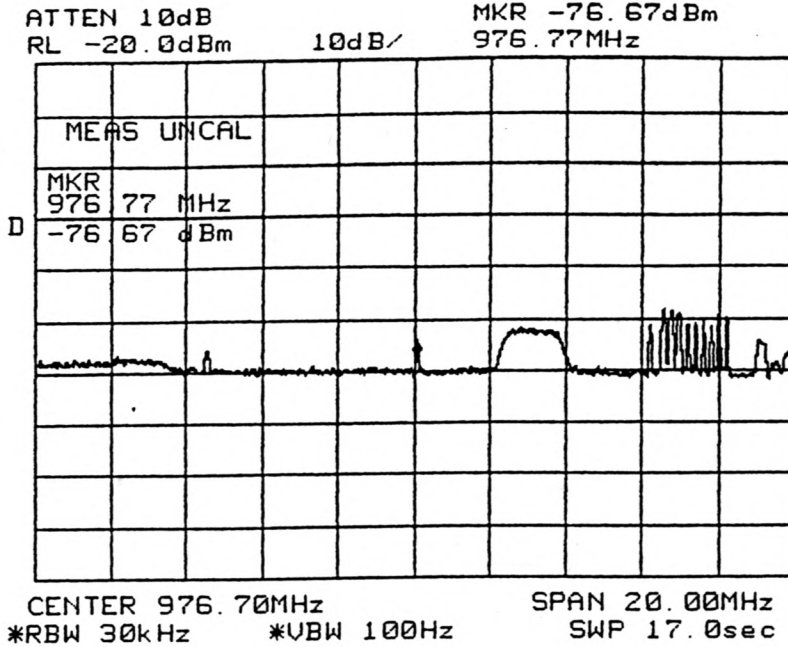
4/7/95

Retrofit of Hawaii Box

- 1) Retuned osc. \rightarrow had shifted \approx 5 mHz lower
- 2) Changed loop components
 - C_4 was 0.01 μ fd \Rightarrow 2 μ fd.
 - C_3 was 0.001 μ fd \Rightarrow Removed
 - $\checkmark R_1$ \Rightarrow 800 Ω (5K pot)
 - $\checkmark R_2$ \Rightarrow 730 Ω (5K pot)
 - $\checkmark R_{13}$ 20K \Rightarrow 40K
 - R_9 3.9M \Rightarrow Same
 - R_7 47K \Rightarrow Same
 - R_6 43K \Rightarrow Same
 - $\checkmark C_{12}$ \Rightarrow 1 μ fd
Nom
- 3) Changed Lock detect from output of AD741 to 74LS94 output
- 4) Added connectors to PLL PCB
- 5) Removed pad + added 50 Ω term to 21.395 MHz splitter
- 6) Changed V_{PLL} monitor resistors to 191K + 590K

5/25/95

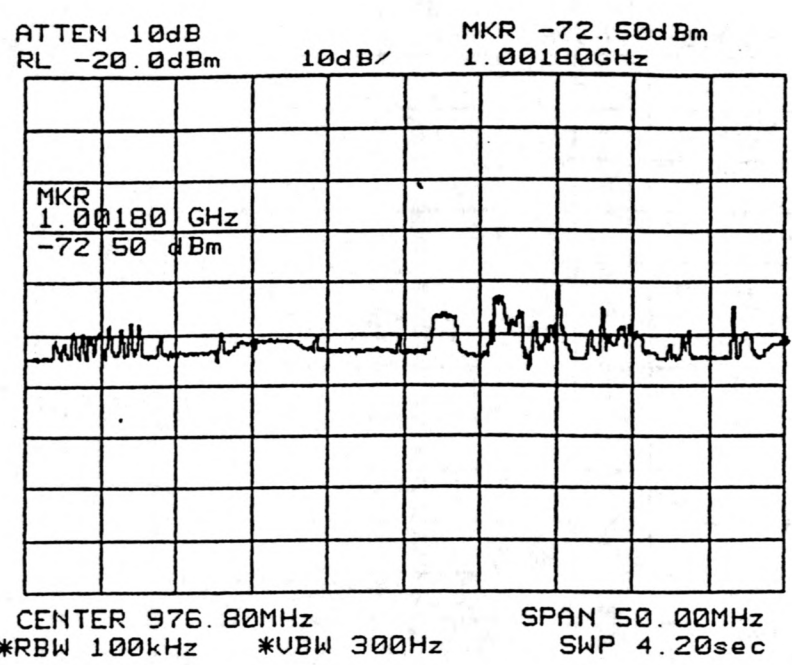
Cstan 4



Locks f_0 : V_E
 $f_{VCO} = 965.8 (-11.0V)$
 $f_{VCO}^* = 961.9 (-7.02)$

5/25/95

G-star 4



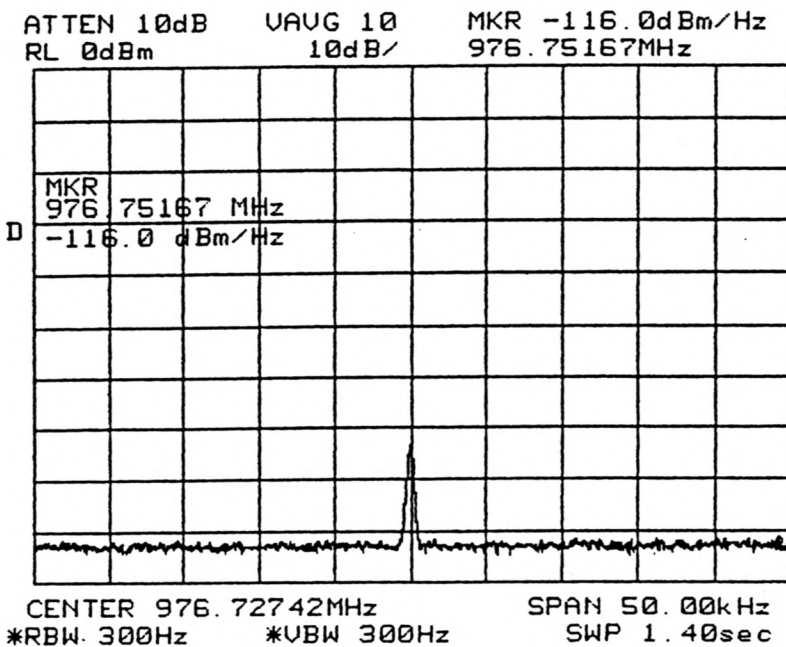
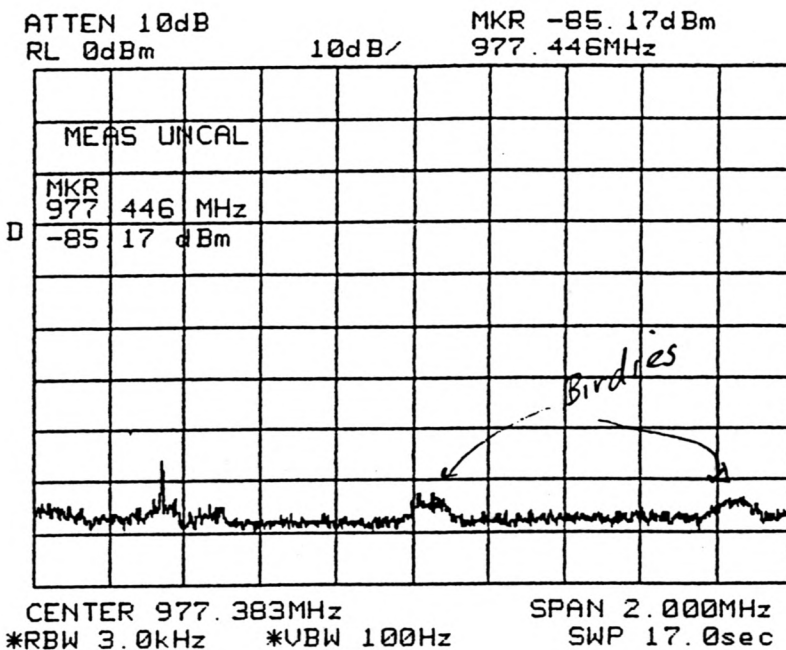
5/26/95

mmA - Hawaii ELEC. BOX

PATIO TEST RANGE

GSTAR 4

~ opposite polarization



ATTEN 20dB UAUG 50 MKR -37dBm

Appendix C
Operation of the AC Power Interrupter

At the time of this writing (March 1999) an AC power interrupter is installed to interrupt power to the interferometer back end electronics to reset the PLL and the computer for a hard reboot. A Black Box Corporation Tone Operated Power Switch is connected to the telephone line and the AC power to the electronics and computer.

To interrupt power:

1. Call the T.O.P.S. on the telephone (x 7054).
2. Enter the access code when prompted.
3. The device will list each outlet number and its on or off state. The electronics/PLL is on outlet 2, the computer is on outlet 4.
5. To turn off the PLL (outlet 2) press 4. To turn the PLL back on press 3.
6. To turn off the computer (outlet 4) press 8. To turn the computer back on press 7.
7. For each number entered the box will respond with which outlet was turned off or on.
8. Entering # will cause the box to list the state of each outlet.
9. Entering * will cause the box to respond with 'Goodbye' and hang up.